Industrial Catalysts

DOI: 10.1002/ange.200463045

Tailored Catalytic Propene Trimerization over Acidic Zeolites with Tubular Pores**

Johan A. Martens, Wim H. Verrelst, Georges M. Mathys, Stephen H. Brown, and Pierre A. Jacobs*

Oligomerization of short alkenes is applied in large-scale petrochemical processes for a variety of products including liquid hydrocarbon fuels, lubricants, detergent precursors, solvents, and plasticizers.[1–4] Whereas longer-chain linear alkenes result from homogeneous catalytic processes that use transition metal complexes,[5] chain-branched alkenes in the C_6–C_{12} range stem from the oligomerization of C_3 or C_4 alkenes using a fixed bed of silica-supported phosphoric acid (SSPA),[1–4,6] at temperatures and pressures amounting to about 520 K and 12 MPa, respectively.[7,8] Despite drawbacks related to the maintenance of a critical feed hydration level, catalyst clogging, and corrosion problems caused by phosphoric acid leaching, SSPA processes are still widely operated.[1–4] We have now discovered that acidic ZSM-22 zeolite allows the synthesis of propene trimers of intermediate degree of chain branching, suitable as feedstock for oxyfunctionalization processes. The narrow tubular pores of this zeolite impose preferential formation of the slimmer linear and monobranched oligomers. Though the in-time stability of ZSM-22 is similar to that of SSPA, the former catalyst does not present the numerous disadvantages encountered with the latter.

Difficulties in finding a viable substitute for SSPA are not only related to the fact that cheap, impure alkene feedstocks are used, but also to the critical product specification with respect to molecular weight and chain branching of the oligomers. Acidic zeolites through their molecular shape selectivity properties can meet these stringent catalyst requirements. For fuel and lubricant applications, a technology based on ZSM-5 has been developed.[9] More recently, ZSM-57 with its unique lobate pore structure was reported to be a stable and selective dimerization catalyst for C_4–C_6 alkenes.[10] With a ZSM-57-type catalyst, the number of chain branchings (NCB) of the alkene dimers is high and similar to that of processes using SSPA. In oxyfunctionalization processes, olefins with two and especially with three or more chain branchings show decreased reactivity.[11] We now report the advantageous use of ZSM-22 for the synthesis of propene trimers with appropriate low NCB.

Zeolite pore architecture is characterized by the dimensionality and size of the channel system, the latter being determined by the number of oxygen atoms in the ring circumscribing the opening. Candidate zeolite topologies categorized according to micropore architecture were screened in the propene trimerization reaction using a mixture of 12 wt % of propene in propane fed in supercritical state at 6.8 MPa and 473–513 K. Contact time was adapted to reach at least initially a high conversion level. With respect to trimerization yield (Y_{C9}) and limitation of NCB, zeolites with a tubular 10-membered ring (10-MR) channel system devoid of large lobes or intersections outperformed all others (Figure 1, bottom). On the majority of zeolite structure types known today, with intersecting 10-MR channels, side pockets, or pronounced lobes or with 12-MRs,[12] Y_{C9} at high conversion was reduced, while the NCB was close to 2.0 (Figure 1, top), a value typical for SSPA processes.

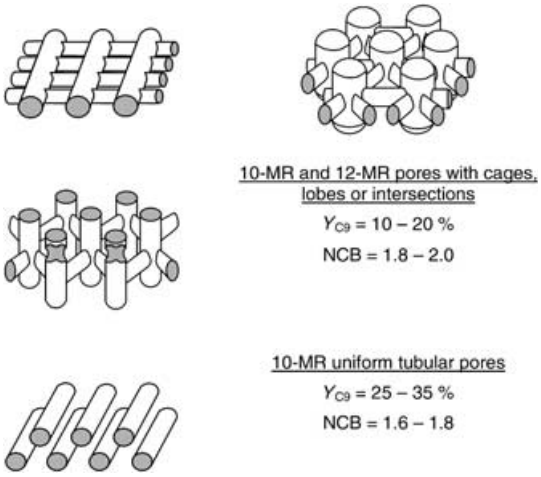

Figure 1. Influence of the micropore system of the acidic zeolite at propene conversions exceeding 80% on propene trimer yield (Y_{C9}) and number of chain branchings (NCB).

Uniform 10-MR tubular pores are encountered in ZSM-22, ZSM-23, SAPO-11 with TON, MTT, and AEL topology, respectively,[12] as well as in the ZSM-48 family of zeolites.[13,14] With ZSM-22, initially all propene was converted. Though the activity showed some decay with time-on-stream, an amount of propene corresponding to 400 times the catalyst weight could be converted easily (see Experimental Section). The three other zeolites showed decreased initial activity, with similar (ZSM-23) or higher rates of decay (ZSM-48 and SAPO-11).

Under the presently used reaction conditions, typical for industrial processes, the tubular 10-MR zeolite catalysts yielded mainly dimers, trimers, and tetramers as reaction products. This is evident from Figure 2, which also clearly

[*] Prof. J. A. Martens, Dr. W. H. Verrelst, Prof. P. A. Jacobs
Centre for Surface Chemistry and Catalysis
Catholic University of Leuven
Kasteelpark Arenberg 23, 3001 Leuven (Belgium)
Fax: (+32) 16-32-19-98
E-mail: johan.martens@agr.kuleuven.ac.be
Dr. G. M. Mathys, Dr. S. H. Brown
ExxonMobil Chemical Europe, Inc.
European Technology Center
Hermeslaan 2, 1831 Machelen (Belgium)

[**] J.A.M. and P.A.J. acknowledge the Flemish Government for support in the frame of a Concerted Research Action on Catalysis (GOA), as well as the Federal Services of Science Policy for support in the frame of a IAP-PAI Network on Supramolecular Catalysis.

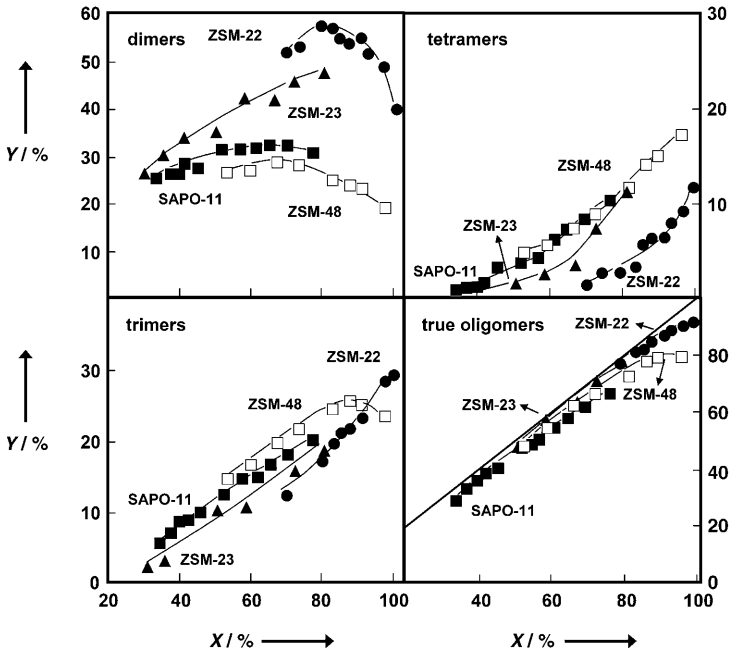

Figure 2. Yield (*Y*) of propene dimers, trimers, tetramers, and of total true oligomers (di- to hexamers, without products with intermediate carbon numbers obtained by cracking and recombination of fragments) against propene conversion (*X*) with ZSM-22, ZSM-23, ZSM-48, and SAPO-11.

indicates that on all four catalysts the true oligomers remain the largest product fraction up to high conversion—for ZSM-23 and ZSM-22 even more pronounced than for SAPO-11 and ZSM-48. Despite the high conversion, also oligomer chain growth was limited. On ZSM-22, the dimer yield peaked at around 80% propene conversion; the trimer yield close to 100% (Figure 2). The highest trimer yields were obtained with ZSM-22. Chain growth was more pronounced on ZSM-23, SAPO-11, and ZSM-48, as noted from the more abundant formation of tetramers and the occurrence of dimer and trimer yield maxima at lower propene conversion.

Given the multitude of possible double-bond and skeletal isomers, the molecular reaction network for propene oligomerization is complex. As double bond positions in the individual dimers were always at equilibrium, selectivity discussions can be limited to the rationalization of the branching of the alkane skeleton obtained after saturation of the double bond. Chain branching was analyzed using gas chromatography with sample hydrogenation (see Experimental Section). In the dimer fraction obtained on ZSM-22 (Figure 3), primary products dominating at low conversion have a carbon skeleton with a methyl branch at C2, as expected for an acid-catalyzed alkylation [Eq. (1)].

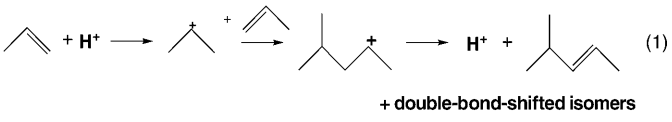

(1)

Skeletal isomers with methyl branching at C3 are secondary products obtained by methyl shifts on 2-methyl-

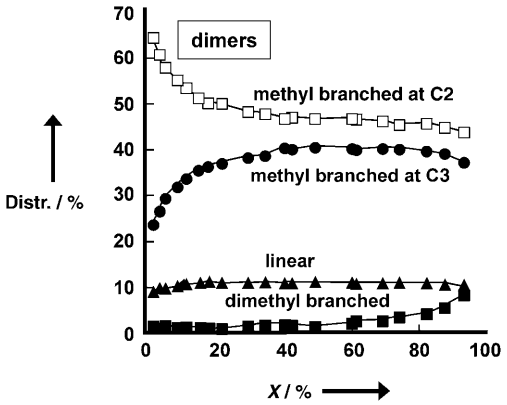

Figure 3. Skeletal distribution of the dimer fraction obtained at increasing propene conversion with ZSM-22.

branched isomers (Figure 3). With ZSM-22, methyl shifts on alkylcarbenium ions were found to be substantially slower than de-branching reactions in which one branch vanishes.[15] Linear dimers observed over the entire conversion range (Figure 3) stem from fast de-branching reactions of 2-methylpentenes. Above 40% propene conversion, linear and methyl-branched dimers are found at equilibrium with ZSM-22 as catalyst (Figure 3). Dimers with dimethyl-branched carbon skeleton were obtained only at high feed conversion. Similar dimers fractions were obtained on the other 10-MR tubular zeolites, except for the more pronounced formation of dibranched dimers on SAPO-11 and ZSM-48.

The NCB in the trimer fractions obtained with 10-MR tubular zeolites is displayed in Figure 4 and compared with that of a typical trimer fraction obtained on SSPA, representative for an oligomerization without any confinement in micropores. The large majority of trimers show a dibranched carbon skeleton (Figure 4), which can be explained by acid-catalyzed oligomerization causing an additional branching upon addition of a novel propene unit to a methyl-branched dimer. Especially with ZSM-23 and ZSM-22, the fraction of

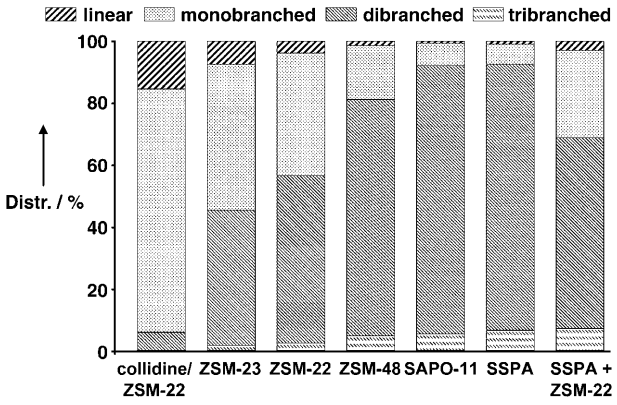

Figure 4. Skeletal distribution of trimer fractions at 30% propene conversion, obtained on collidine-treated ZSM-22, ZSM-23, ZSM-22, ZSM-48, SAPO-11, SSPA, and on successive layers of SSPA and ZSM-22.

trimers with monobranched or linear carbon skeleton is larger than with SSPA. Propene trimers are methyl-branched at carbon positions 3 and 4 (3,4-group isomers) unless the branchings are shifted (2,6-group isomers) or eliminated to give monobranched and linear isomers (monobranched-group isomers).[16] Among the 10-MR tubular pore zeolites the formation of monobranched-group nonene isomers decreases in the series ZSM-23 > ZSM-22 > ZSM-48 > SAPO-11 (Figure 5). The skeletal distribution of the trimer fraction obtained with SAPO-11 is already very similar to that encountered with SSPA (Figure 4).

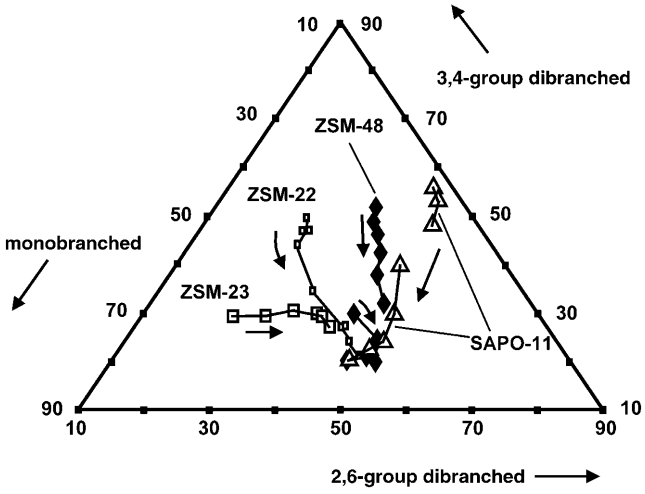

Figure 5. Compositional diagram showing the evolution of the skeletal structures of propene trimers obtained with 10-MR tubular pore zeolites at increasing conversions indicated by the arrows.

Among the known zeolite structure types, those with tubular 10-MRs having a free diameter of around 0.5 nm exhibit the highest heats of adsorption for linear hydrocarbons.[17–22] The free diameters of ZSM-23 pores of $0.45 \times 0.52\ nm^2$ [12] preclude methyl-branched alkanes from entering.[17] The penetration of the same methyl-branched alkanes into the slightly wider ZSM-22 pores with cross sections of $0.44 \times 0.55\ nm^2$ is possible, depending on conditions.[17–20] SAPO-11 belongs to the AEL zeolite family, has a little wider 10-MR of $0.40 \times 0.65\ nm^2$, and readily adsorbs isoalkanes.[21,22] Sorption data on ZSM-48 with its relatively wide 10-MR of $0.53 \times 0.56\ nm^2$ are not available. Catalytic test reactions such as the determination of the constraint index[23] and of the refined constraint index[24] reveal that there is less steric limitation inside SAPO-11 and ZSM-48 pores than inside ZSM-22 and ZSM-23 pores. Thus the observed tendency of debranching of propene trimers in the zeolite sequence of SAPO-11 < ZSM-48 < ZSM-22 < ZSM-23 (Figures 4 and 5) reflects the order of decreasing effective pore width.

The stronger limitation of oligomer chain growth in ZSM-22 compared with ZSM-23 (Figure 2) can be explained as follows: Inside the pores of these two zeolites, the formation of tetramers most likely occurs through propene addition to linear trimers. As ZSM-23 exhibits a stronger tendency to trimer linearization, it shows a more pronounced chain growth. In ZSM-48 and SAPO-11, chain growth can probably also proceed on monobranched trimer chains, explaining why in these zeolites tetramer formation is also more pronounced than in ZSM-22.

As the ZSM-22 crystals are micrometer-sized and the specific external surface area amounts to about $40\ m^2 g^{-1}$, pore mouth sites of ZSM-22 may contribute significantly to catalysis, for example, in catalytic isodewaxing.[25] Acidic sites on the external surfaces and pore mouths of ZSM-22 can be selectively poisoned with collidine (2,4,6-trimethylpyridine), a bulky amine that cannot penetrate the pores of 10-MR zeolites. Whereas the collidine-poisoned ZSM-22 catalyst was about five times less active than the parent sample, the trimer fraction was very rich in monobranched nonenes (80%) and contained a significant amount of linear nonenes (15%) (Figure 4), confirming that catalytic sites located inside the tubular pores are responsible for the formation of monobranched and linear trimers, and that sites accessible to collidine are responsible for the formation of di- and tribranched nonenes. ZSM-22 also shows "coke selectivation" as partially deactivated catalysts were found to be more selective for linear and monobranched nonenes than fresh catalysts, owing to a gradual loss of the contribution of the external sites.

ZSM-22 can be used as hydroisomerization catalyst for converting long-chain *n*-alkanes into mono- and dibranched skeletal isomers,[25] as it establishes the internal equilibrium between the linear alkane, its monobranched isomers, and specific dibranched isomers.[25] This property of ZSM-22 can be exploited to reduce the NCB of the C_9 products obtained from propene oligomerization with SSPA as was shown for the trimer fraction produced in a process with SSPA for which the NCB was reduced from 2.0 to 1.7 during a typical catalytic run (473 K, 6.8 MPa, $W/F_0 = 280\ kg\,s\,mol^{-1}$). The reduction resulted primarily from conversion of dibranched into monobranched and linear nonenes (Figure 4, columns 6 and 7). Tribranched isomers have too little adsorption affinity in pore mouths and are not converted. Dibranched isomers undergo a first de-branching in pore mouths and eventually entire linearization deeper inside the pores.

The ZSM-22 catalysis was also run using feedstock of 50 wt% propene in propane, similar to a process with SSPA. Though with this propene-rich feed, pronounced exothermicity in the catalyst bed was observed, deactivation was minor. Propene conversion remained complete until an amount of propene of at least 400 times the catalyst weight was fed. An incremental increase of catalyst temperature was sufficient to reestablish complete propene conversion. Finally, the experiment was interrupted after the formation of more than 600 kg of oligomer product per kg of catalyst, which is in the range of oligomer yields with SSPA processes. ZSM-22 also brings an important environmental benefit, as it is reusable many times after regeneration and has a much longer lifetime than SSPA which can only be used once. Thus, the use of ZSM-22 in propene oligomerization adds to the sustainability of the petrochemical industry.

Experimental Section

Zeolite samples were synthesized according to published methods: ZSM-22,[26] ZSM-23 was run 4 of reference [27], ZSM-48,[28] SAPO-11[29] was sample S-11/2 of reference [30]. The Si/Al ratio of ZSM-22, -23, and -48 was 42, 44, and 50, respectively. The phase purity was confirmed by XRD and SEM. Gram quantities of as-synthesized zeolite powder were pelletized (0.25–0.50 mm) by compression, loaded in a quartz tube, and calcined, first under flowing nitrogen at 400 °C for 5 h and subsequently under oxygen at 550 °C for 15 h. The samples were exchanged with 0.5 M aqueous NH_4Cl solution and calcined at 400 °C. This procedure resulted in acidic zeolites with more than 99.5 % of the aluminum tetrahedrally coordinated according to ^{27}Al MAS-NMR (signal at 54 ppm against aluminum nitrate reference with a Bruker Avance 400 MHz instrument; spinning frequency of 20 kHz). The FT-IR spectra of the zeolites displayed absorptions at about 3595 and 3745 cm^{-1}, assigned to bridging Al–OH–Si groups with Brønsted acid character and framework-terminating silanol groups, respectively. IR absorption bands at about 3655 cm^{-1}, which are characteristic of hydroxy groups on aluminum atoms that are partially dislodged from the framework and responsible for Lewis acidity, were absent.

The chemical composition of the SAPO-11 material corresponds to $(Si_{0.21}Al_{0.43}P_{0.36})0_2$. The SAPO-11 crystals are composed of 28 % aluminosilicate (AS) and 72 % silicoaluminophosphate (SAP) domains.[30] The catalytic activity of SAPO-11 is mainly due to Brønsted acid sites at the interphase between the AS and SAP domains.

Catalytic experiments in a fixed-catalyst-bed continuous-flow reactor: catalyst pellets of compressed zeolite powder with diameters of 0.25–0.50 mm were loaded in a stainless steel reactor tube with an internal diameter of 9 mm and a length of 300 mm. Empty volume was filled with alumina beads of the same diameter. Reaction conditions: $T = 473$ K; $P = 6.8$ MPa; feedstock: 12 wt % propene in propane; $W/F_0 = 34$ kg s mol^{-1} (W: catalyst weight; F_0: molar propene flow at reactor inlet); liquid feedstock delivered with a liquid mass flow controller (Brooks Instruments). The reactor outlet was sampled online at high pressure using a 4-port HPLC sampling valve (Valco) with an internal volume of 0.1 μL, and analyzed with capillary gas chromatography. Product NCB was determined offline on a gas chromatograph with sample hydrogenation module.

Received: December 23, 2004
Revised: February 23, 2005
Published online: August 1, 2005

Keywords: oligomerization · propene · shape selectivity · silica-supported phosphoric acid · zeolites

[1] K. Tanabe, W. F. Höldrich, *Appl. Catal. A* **1999**, *181*, 399 – 434.
[2] K. Weissermel, H. J. Arpe, *Industrial Organic Chemistry*, 4th ed., Wiley-VCH, Weinheim, **2003**, pp. 83 – 85.
[3] S. Matar, L. F. Hatch, *Chemistry of Petrochemical Processes*, 2nd ed., Butterworth-Heinemann, Woburn, MA, **2001**, chap. 8.
[4] D. York, J. C. Scheckler, D. G. Tajbl in *Handbook of Petroleum Refining Processes*, 3rd ed. (Ed.: R. A. Meyers), McGraw-Hill, New York, **2003**, pp. 1.21 – 1.30.
[5] J. Skupinska, *Chem. Rev.* **1991**, *91*, 613 – 648.
[6] V. N. Ipatieff, B. B. Corson, G. Egloff, *Ind. Eng. Chem.* **1935**, *27*, 1077 – 1081.
[7] K. G. Wilshier, P. Smart, R. Western, T. Mole, T. Behrsing, *Appl. Catal.* **1987**, *31*, 339 – 359.
[8] C. T. O'Connor, M. Kojima, *Catal. Today* **1990**, *6*, 329 – 349.
[9] S. A. Tabak, F. J. Krambeck, W. E. Garwood, *AICHE J.* **1986**, *32*, 1526 – 1531.
[10] J. A. Martens, R. Ravishankar, I. E. Mishin, P. A. Jacobs, *Angew. Chem.* **2000**, *112*, 4547 – 4550; *Angew. Chem. Int. Ed.* **2000**, *39*, 4376 – 4379.
[11] B. Cornils in *New Synthesis with Carbon Monoxide* (Ed.: J. Falbe), Springer, Berlin, **1980**, p. 96.
[12] C. Baerlocher, W. M. Meier, D. H. Olson, *Atlas of Zeolite Framework Types*, 5th ed., Elsevier, Amsterdam, **2001**.
[13] J. L. Schlenker, W. J. Rohrbaugh, P. Chu, E. W. Valyocsik, G. T. Kokotailo, *Zeolites* **1985**, *5*, 355 – 358.
[14] R. F. Lobo, H. van Koningsveld, *J. Am. Chem. Soc.* **2002**, *124*, 13222 – 13230.
[15] C. S. L. Narasimhan, J. W. Thybaut, G. B. Marin, P. A. Jacobs, J. A. Martens, J. F. Denayer, G. V. Baron, *J. Catal.* **2003**, *220*, 399 – 413.
[16] After hydrogenation, the 3,4-group comprises the following isomers: 3,4-, 2,3- and 4,4-dimethylheptane; 3-ethyl-2-methyl- and 3-ethyl-3-methylhexane; 2,3,4-trimethylhexane. The 2,6-group comprises 2,6-, 2,5-, 3,5-, 2,4-, and 2,2-dimethylheptane.
[17] J. F. Denayer, A. R. Ocakoglu, W. Huybrechts, J. A. Martens, J. W. Thybaut, G. B. Marin, G. V. Baron, *Chem. Commun.* **2003**, *15*, 1880 – 1881.
[18] M. Schenk, B. Smit, T. J. H. Vlugt, T. L. M. Maesen, *Angew. Chem.* **2001**, *113*, 758 – 761; *Angew. Chem. Int. Ed.* **2001**, *40*, 736 – 739.
[19] F. Eder, J. A. Lercher, *J. Phys. Chem. B* **1997**, *101*, 1273 – 1278.
[20] J. A. Z. Pieterse, S. Veefkind-Reyes, K. Seshan, J. A. Lercher, *J. Phys. Chem. B* **2000**, *104*, 5715 – 5723.
[21] F. Eder, J. A. Lercher, *J. Phys. Chem.* **1996**, *100*, 16460 – 16462.
[22] H. Stach, K. Fiedler, J. Janchen, *Pure Appl. Chem.* **1993**, *65*, 2193 – 2200.
[23] V. J. Frilette, W. O. Haag, R. M. Lago, *J. Catal.* **1981**, *67*, 218 – 223.
[24] P. A. Jacobs, J. A. Martens, *Pure Appl. Chem.* **1986**, *58*, 1329 – 1338.
[25] J. A. Martens, W. Souverijns, W. Verrelst, R. Parton, G. F. Froment, P. A. Jacobs, *Angew. Chem.* **1995**, *107*, 2726 – 2728; *Angew. Chem. Int. Ed. Engl.* **1995**, *34*, 2528 – 2530.
[26] S. Ernst, J. Weitkamp, J. A. Martens, P. A. Jacobs, *Appl. Catal.* **1989**, *48*, 137 – 148.
[27] S. Ernst, R. Kumar, J. Weitkamp, *Catal. Today* **1988**, *3*, 1 – 10.
[28] P. A. Jacobs, J. A. Martens, *Stud. Surf. Sci. Catal.* **1987**, *33*, 22.
[29] M. Mertens, J. A. Martens, P. J. Grobet, P. A. Jacobs in *Guidelines for Mastering the Properties of Molecular Sieves* (Ed.: D. Barthomeuf), Plenum, New York, **1990**, p. 1.
[30] J. A. Martens, P. J. Grobet, P. A. Jacobs, *J. Catal.* **1990**, *126*, 299 – 305.

